ANL-6713

Argonne National Laboratory

CRITICAL STUDIES OF A SMALL URANIUM CARBIDE-FUELED REACTOR WITH A BERYLLIUM REFLECTOR (ZPR-III Assembly 40)

by

R. L. McVean, P. I. Amundson,
G. S. Brunson, and J. M. Gasidlo

ANL-6713
Reactor Technology
(TID-4500, 20th Ed.)
AEC Research and
Development Report

ARGONNE NATIONAL LABORATORY
9700 South Cass Avenue
Argonne, Illinois

CRITICAL STUDIES OF A SMALL URANIUM CARBIDE-FUELED REACTOR WITH A BERYLLIUM REFLECTOR (ZPR-III Assembly 40)

by

R. L. McVean, P. I. Amundson,
G. S. Brunson, and J. M. Gasidlo

Idaho Division

April 1963

Operated by The University of Chicago
under
Contract W-31-109-eng-38
with the
U. S. Atomic Energy Commission

TABLE OF CONTENTS

		Page
ABSTRACT		5
I.	INTRODUCTION	5
II.	REACTOR SIZE AND COMPOSITION	5
III.	SAFETY CONSIDERATIONS	10
IV.	EXPERIMENTAL RESULTS	13
	A. Critical Mass	13
	B. Reactivity Coefficients	13
	C. Fission Traverses	14
	D. Central Fission Ratios	14
	E. Radial Beryllium Reflector Experiments	16
	F. Rossi-alpha Measurements	18
ACKNOWLEDGMENTS		19
REFERENCES		19

LIST OF FIGURES

No.	Title	Page
1.	Horizontal Cross Section of Assembly 40 (Cylindrical Symmetry)	6
2.	Interface Views of Assembly 40	6
3.	Zone I (Core) Drawer Master Loading Chart (Half No. 1)	7
4.	Zone I (Core) Drawer Master Loading Chart (Half No. 2)	8
5.	Zone II Drawer Master Loading Chart (Half No. 1)	8
6.	Zone II Drawer Master Loading Chart (Half No. 2)	8
7.	Zone III Drawer Master Loading Chart (Half No. 1)	9
8.	Zone III Drawer Master Loading Chart (Half No. 2)	9
9.	Zone IV Drawer Master Loading Chart (Half No. 1)	9
10.	Zone IV Drawer Master Loading Chart (Half No. 2)	10
11.	Polyethylene Slab in Place for "Fat Man" Experiment	11
12.	Approach to Critical Curve	11
13.	Calibration of Control Rod No. 10	13
14.	Fissile Sample Locations for Reactivity Coefficient Measurements	14
15.	Nonfissile Sample Location for Reactivity Coefficient Measurements at Core Center	14
16.	Nonfissile Sample Locations for Reactivity Coefficient Measurements at Radial Core Boundary	14
17.	Nonfissile Sample Locations for Reactivity Coefficient Measurements at Axial Core Boundary	14
18.	U^{235} Radial Fission Traverse	15
19.	U^{238} Radial Fission Traverse	16
20.	U^{235} Axial Fission Traverse	16
21.	U^{238} Axial Fission Traverse	16
22.	Worth of Radial Beryllium Reflector Movement	17
23.	Typical Rossi-alpha Measurements	18

LIST OF TABLES

No.	Title	Page
I.	Volume Fractions for Assembly 40	7
II.	Material Densities	7
III.	Reactivity Worth of Axial Reflector (Zone V) Material Replacing Core Material	12
IV.	Reactivity Worths of Control Rods with Beryllium in Axial Reflector	12
V.	Reactivity Coefficient Measurements	15
VI.	Central Fission Ratios	17

CRITICAL STUDIES OF A SMALL URANIUM CARBIDE-FUELED REACTOR WITH A BERYLLIUM REFLECTOR (ZPR-III Assembly 40)

by

R. L. McVean, P. I. Amundson,
G. S. Brunson, and J. M. Gasidlo

ABSTRACT

A small, lightweight, uranium carbide fueled reactor with a beryllium reflector surrounding the core was mocked up as Assembly 40. It was determined that the presence of beryllium in the axial and radial reflectors did not endanger the safe loading and operation of the critical assembly.

The actual experiment consisted of determination of the critical mass, measurement of the reactivity coefficients for a large number of fissile and nonfissile materials, the performance of radial and axial fission traverses, and measurement of central fission ratios. The effectiveness of the radial beryllium reflector as a control mechanism was determined and the Rossi-alpha was measured.

I. INTRODUCTION

Increased interest in space-age applications for nuclear reactors has resulted in the study of the application of small, fast reactors to space propulsion. It has been pointed out[1] that, since there is a premium on low reactor weight, high power density, and very high temperatures, the fast reactor rocket engine offers promise in this field. The same report describes computational studies of beryllium-reflected fast reactors with core structures resistant to high temperatures. This work covers critical experiments with a mockup of an assembly of this general type.

II. REACTOR SIZE AND COMPOSITION

The Zero Power Reactor III (ZPR-III) is a critical facility for the study of various types of fast reactors. A description of the reactor has been given by Cerutti et al.[2]

Assembly 40 contains a cylindrical core, approximately 28 cm high and 28 cm in diameter, with a volume of 17.5 liters. The axial beryllium reflector is adjacent to the core, whereas the radial beryllium reflector is separated from the core by a low-density region of sodium, molybdenum, stainless steel, and void. The horizontal cross section of the reactor, shown in Fig. 1, locates the various regions mocked up in the assembly. Zone I is the core region, Zone III is the radial beryllium reflector, and Zone V is the axial beryllium reflector. The interface views of the assembly are shown in Fig. 2. Table I lists the volume fractions of the many regions; Table II gives the material densities used in calculating the volume fractions.

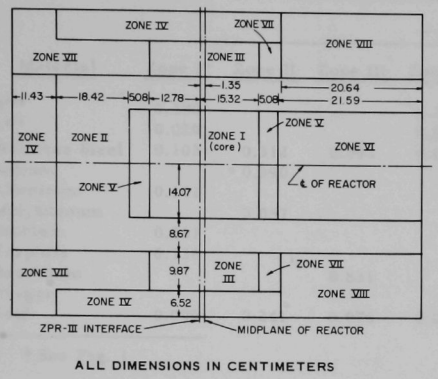

Fig. 1. Horizontal Cross Section of Assembly 40 (Cylindrical Symmetry)

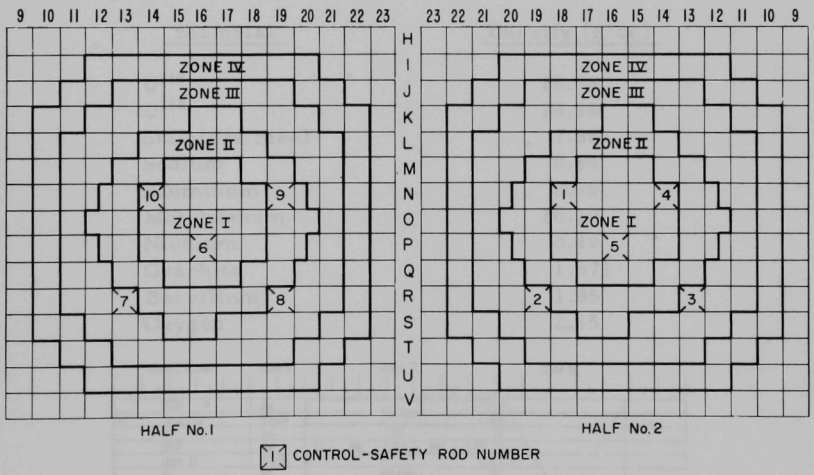

Fig. 2. Interface Views of Assembly 40

It will be noted from Fig. 1 that the assembly loading is not symmetrical around the assembly interface. The basic drawer master loading charts for each half of the assembly are shown in Figs. 3 through 10.

Table I

VOLUME FRACTIONS FOR ASSEMBLY 40

Material	Volume Fractions							
	Zone I*	Zone II	Zone III	Zone IV	Zone V	Zone VI	Zone VII	Zone VIII
U^{235}	0.280			0.002				
U^{238}	0.020			0.833				
Stainless Steel	0.103	0.312	0.093	0.092	0.090	0.214	0.093	0.686
Sodium		0.390				0.761		
Aluminum	0.101				0.152		0.085	
Molybdenum		0.057			0.254			
Niobium	0.261							
Graphite	0.136							
Beryllium			0.831		0.260			
Oxygen					0.143			
Void	0.099	0.241	0.076	0.073	0.101	0.025	0.822	0.314

* See Fig. 1

Table II

MATERIAL DENSITIES

Material	Density (g/cc)
U^{235}	18.72
U^{238}	18.96
Stainless Steel	7.86
Sodium	0.84
Aluminum	2.70
Molybdenum	10.20
Niobium	8.40
Graphite	1.671
Beryllium	1.85
Oxygen	2.55

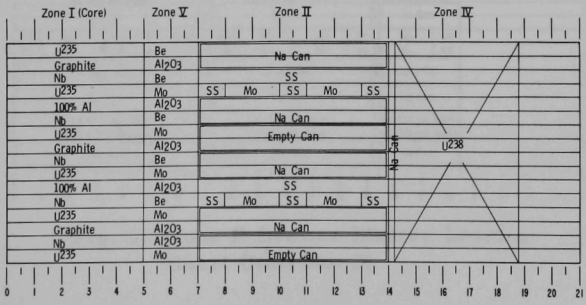

Fig. 3. Zone I (Core) Drawer Master Loading Chart (Half No. 1)

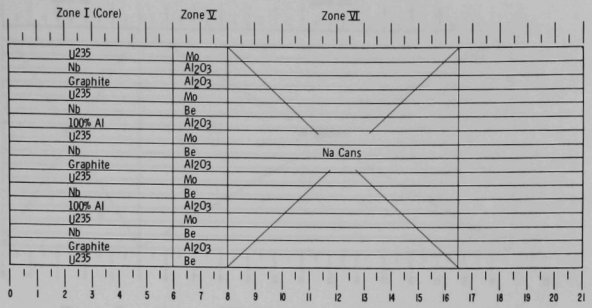

Fig. 4. Zone I (Core) Drawer Master Loading Chart (Half No. 2)

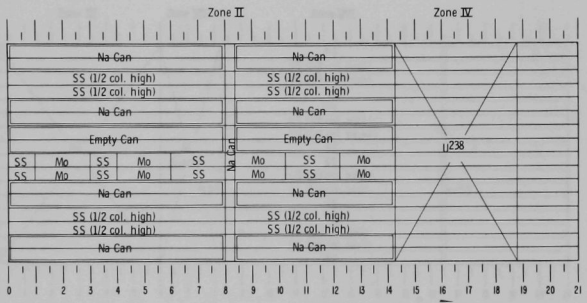

Fig. 5. Zone II Drawer Master Loading Chart (Half No. 1)

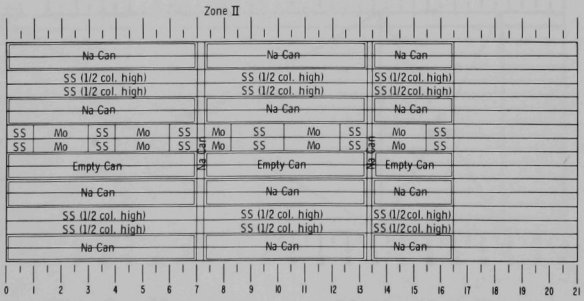

Fig. 6. Zone II Drawer Master Loading Chart (Half No. 2)

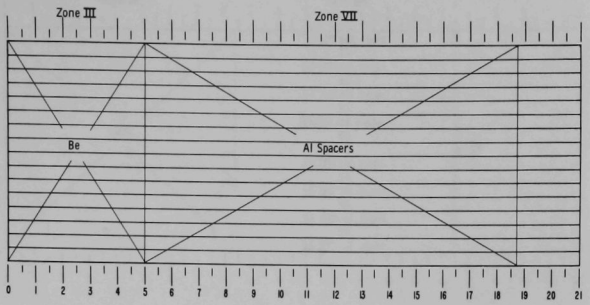

Fig. 7. Zone III Drawer Master Loading Chart (Half No. 1)

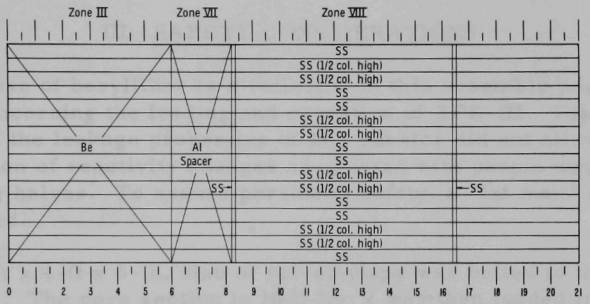

Fig. 8. Zone III Drawer Master Loading Chart (Half No. 2)

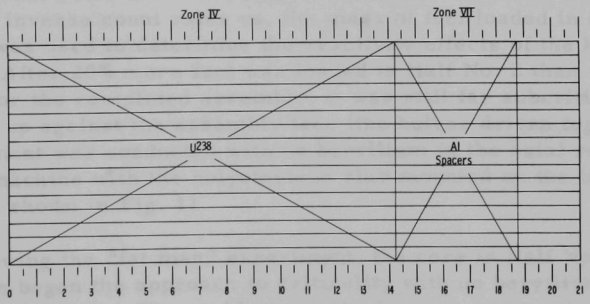

Fig. 9. Zone IV Drawer Master Loading Chart (Half No. 1)

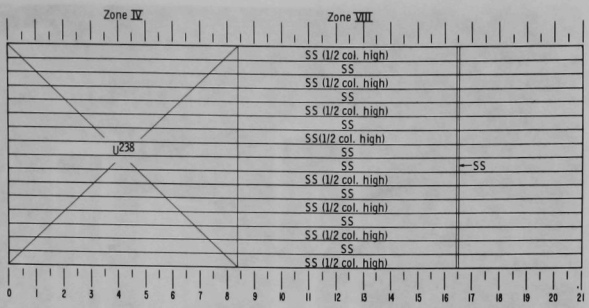

Fig. 10. Zone IV Drawer Master Loading Chart (Half No. 2)

III. SAFETY CONSIDERATIONS

The use of beryllium as a reflector in this assembly posed safety problems concerning the loading and operation of ZPR-III. The limited knowledge of the leakage properties of this reactor did not allow a reasonable prediction of reactivity changes associated with people working between the assembly halves. To assure personnel safety, a "fat man" experiment was conducted.

A 4-ft x 4-ft x 6-in. slab of polyethylene was bolted to the front face of Half No. 1. The core section in Half No. 2 was then loaded in increments. Each time an increment of fuel was added, the halves were run together, placing the polyethylene against the interface of Half No. 2. The subcritical count rates from three different counters were then recorded. A plot of the inverse count rates vs. the mass of fuel loaded in one half of the reactor was used to determine the reactivity effects of the hydrogenous moderator. After 20% more fuel was loaded in Half No. 2 than was expected in that half for the completed assembly, it was still far subcritical with the polyethylene up against the assembly face (the halves driven together). This experiment was conducted with no beryllium in the axial reflector. A view of the machine with the polyethylene slab mounted on the interface of Half No. 1 is shown in Fig. 11.

Following the "fat man" experiment, the core in Half No. 2 was unloaded. Then began the approach to criticality with no beryllium in either of the axial reflectors. Figure 12 shows the inverse count rates vs. the mass of fuel loaded during the approach to criticality. The bending down of the curves is due to the moderating effect of the radial beryllium reflector, which increases the fuel worth at the radial edge of the core. The critical mass of this configuration was approximately 95 kg of U^{235}.

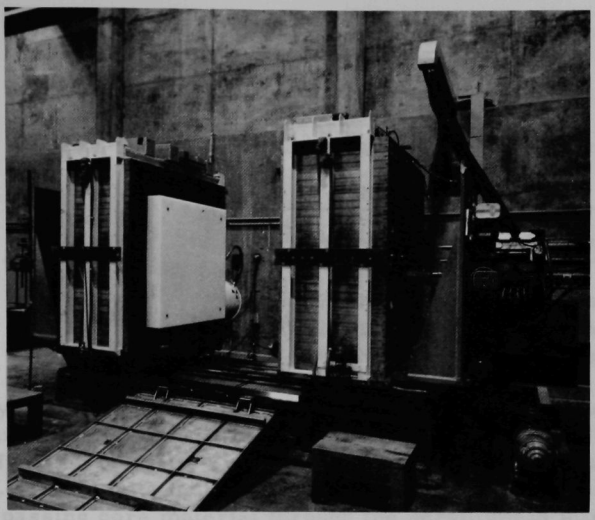

Fig. 11. Polyethylene Slab in Place for "Fat Man" Experiment

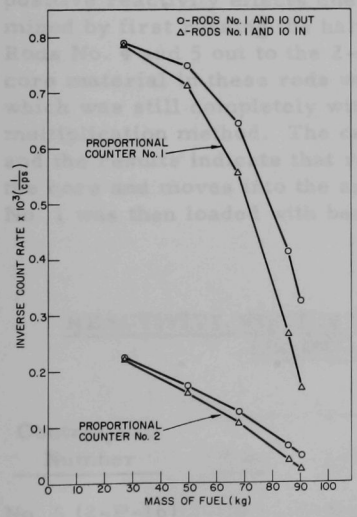

Fig. 12. Approach to Critical Curve. (Beryllium in Axial Blanket)

The reactivity effects of replacing 2 in. of core material with Zone V (axial reflector) material containing beryllium, at various positions in a drawer, was then determined along the core axis and also axially near the core boundary. The results, listed in Table III, were negative in all cases, showing that one core drawer at a time containing beryllium in Zone V could be safely inserted or removed from the matrix.

The situation in which all the safety rods simultaneously pass through the axial beryllium reflector, Zone V, as on a scram, was considered quite uncertain and potentially hazardous. In this situation, the enriched material of the core safety rods must pass through the partial-density beryllium, momentarily forming a lattice configuration which has uncertain multiplication properties.

Table III

REACTIVITY WORTH OF AXIAL REFLECTOR (ZONE V) MATERIAL REPLACING CORE MATERIAL

Position in Drawer, in.	Drawer Number 2-O-16	2-P-14
0 to 2	-375 Ih	-145 Ih
2 to 4	-320 Ih	-122 Ih
4 to 6	-187 Ih	- 87 Ih

Beryllium was first added in Zone V in the four drawers surrounding the central safety-control rod (Rod No. 5) in Half No. 2. The reactivity worth as a function of position of this rod was then measured and is shown in Table IV. The results indicated no net positive reactivity effects associated with passing core material through the beryllium in this case. This procedure was extended to include the three safety-control rods located in the core of Half No. 2. When the beryllium was completely loaded in the axial reflector of Half No. 2, it was determined that there would be no net positive reactivity effects due to scramming of the rods. This was determined by first running the halves of the reactor together and then backing Rods No. 4 and 5 out to the 2-in. position. This positioned the last 2 in. of core material in these rods within the axial reflector. Next, Rod No. 1, which was still completely withdrawn, was calibrated by the subcritical multiplication method. The calibration of Rod No. 1 is shown on Table IV, and the results indicate that reactivity will be reduced when the rod leaves the core and moves into the axial reflector. The axial reflector in Half No. 1 was then loaded with beryllium.

Table IV

REACTIVITY WORTHS OF CONTROL RODS WITH BERYLLIUM LOADED IN AXIAL REFLECTOR

Control Rod Number	Rod Position 0 in.	1 in.	2 in.	4 in.	6 in.	8 in.
No. 5 (2-P-16)	0	-145 Ih	-295 Ih	-575 Ih	-800 Ih	-925 Ih
No. 1 (2-N-18)	0		-165 Ih	-320 Ih	-440 Ih	-520 Ih

IV. EXPERIMENTAL RESULTS

A. Critical Mass

The next step following the complete loading of beryllium in both axial reflectors was to determine the critical mass. The reactor was 187.9 Ih supercritical with a loading of 93.35 kg of U^{235} in the core at a matrix temperature of 22.5°C. Subsequent measurements found the worth of fuel at the core edge to be 113.0 Ih/kg of U^{235}. Therefore, the critical mass with this configuration was 91.89 kg of U^{235} as compared with a calculated value of 88 kg. The calibration curve of the control rod for this loading is shown in Fig. 13.

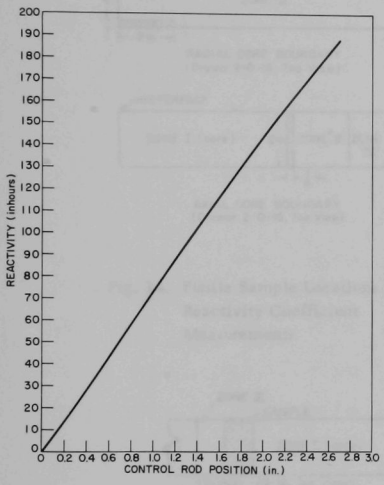

Fig. 13. Calibration of Control Rod No. 10

B. Reactivity Coefficients

Measurements of reactivity worth relative to void were made for fissile and nonfissile materials at the core center, radial core boundary, and axial core boundary.

Only one sample was used for each of the fissile material measurements. The sample was 2 x 2 x $\frac{1}{4}$ in. in size, and was either clad in aluminum or sandwiched between solid aluminum plates. By using perforated aluminum plates in the reference loading, the substitution was made with a negligible change of aluminum. The measurements for the core center were made in the front of drawer 2-O-16, the radial core boundary measurements were made in 2-O-19, and the axial core boundary measurements were made in 2-O-16. Figure 14 shows the positions of the samples in these three drawers.

The nonfissile samples of material, except for $B_4^{10}C$ and polyethylene, were 1 x 2 x 2 in. in size. All central core measurements were made with only one 4-in.^{3} sample at the front of drawer 2-O-16. One sample of material was used for a few measurements at the radial core boundary in 2-O-19. The remaining materials were measured using two samples, one in 2-O-19 and one in 2-R-16. All axial core boundary measurements were made with the two samples, one in 1-O-16 and one in 2-O-16. Figures 15, 16, and 17 show the sample locations in these drawers. Table V lists the results of all reactivity coefficient measurements. An uncertainty of ± 1 Ih has been assumed for these measurements.

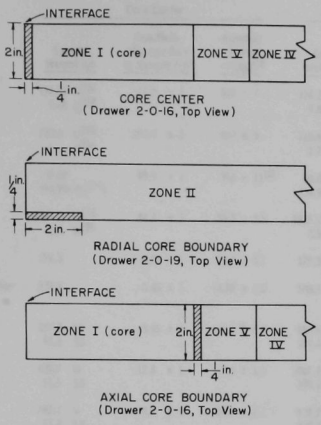

Fig. 14. Fissile Sample Locations for Reactivity Coefficient Measurements

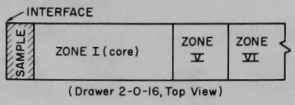

Fig. 15. Nonfissile Sample Location for Reactivity Coefficient Measurement at Core Center

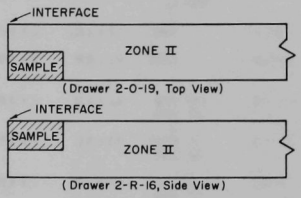

Fig. 16. Nonfissile Sample Locations for Reactivity Coefficient Measurements at Radial Core Boundary

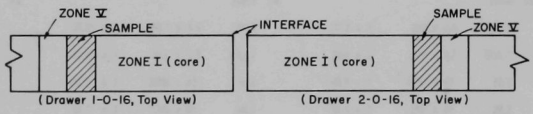

Fig. 17. Nonfissile Sample Locations for Reactivity Coefficient Measurements at Axial Core Boundary

C. Fission Traverses

Fission traverses were made with the use of U^{235} and U^{238} fission counters. These counters were 2 in. long and $\frac{1}{2}$ in. in diameter. Radial traverses were made through the core and reflector at the reactor midplane. Axial traverses were made through the center of the reactor. The results are plotted in Figs. 18, 19, 20, and 21 with the count rates normalized to unity at the center of the core.

D. Central Fission Ratios

Central fission ratios were measured with the aid of absolute fission counters.[3] The data were obtained by placing one fission counter containing a fissionable isotope at the center of the core. The counting rate was obtained relative to a fixed fission counter at the core boundary. The counting rates for all the central fission counters were then normalized through use of the fixed counter at the core boundary.

Table V

REACTIVITY COEFFICIENT MEASUREMENTS FOR ASSEMBLY 40

Material	Core Center			Radial Core Boundary			Axial Core Boundary		
	Sample Weight (g)	Reactivity Change Due to Sample (1h)	Material Worth (1h/kg)[3]	Sample Weight (g)	Reactivity Change Due to Sample (1h)	Material Worth (1h/kg)[3]	Sample Weight (g)	Reactivity Change Due to Sample (1h)	Material Worth (1h/kg)[3]
U^{235}	134.21 U^{235} 9.68 U^{238}	71.2 ± 1	527 ± 7	134.21 U^{235} 9.68 U^{238}	20.3 ± 1	150 ± 7	134.21 U^{235} 9.68 U^{238}	26.5 ± 1	195 ± 7
U^{233}	110.6 U^{233} 2.7 U^{238}	104.0 ± 1	940 ± 9	110.6 U^{233} 2.7 U^{238}	30.8 ± 1	278 ± 9	110.6 U^{233} 2.7 U^{238}	38.5 ± 1	348 ± 9
Pu^{239}	93.02 (94.5% Pu^{239})	89.1 ± 1	958 ± 11[4]	93.02 (94.5% Pu^{239})	21.3 ± 1	229 ± 11[4]	93.02 (94.5% Pu^{239})	31.2 ± 1	335 ± 11[4]
U^{238}	1215.2 U^{238} 2.5 U^{235}	44.3 ± 1	35.3 ± 0.8	1215.2 U^{238} 2.5 U^{235}	29.1 ± 1	23.6 ± 0.8	2430.4 U^{238} 5.0 U^{235}	90.8 ± 1	36.9 ± 0.4
Al	175.3	4.55 ± 1	26.0 ± 5.7	175.3	19.9 ± 1	113.5 ± 5.7	331.7	51.9 ± 1	156.2 ± 3.0
Stainless Steel (SS)	508.3	-0.40 ± 1	-0.80 ± 2.0	508.3	17.7 ± 1	34.8 ± 2.0	1016.6	69.4 ± 1	68.3 ± 1.0
Nb	239.9 Nb 51.1 SS	-3.95 ± 1	-16.3 ± 4.2	489.6 Nb 102.4 SS	26.6 ± 1	47.1 ± 2.0	489.6 Nb 102.4 SS	43.7 ± 1	74.9 ± 2.0
W	920.7 W 51.5 SS	-12.8 ± 1	-13.9 ± 1.1	1867.2 W 103.1 SS	25.8 ± 1	12.0 ± 0.5	1867.2 W 103.1 SS	63.3 ± 1	30.1 ± 0.5
V	267.7 V 51.3 SS	9.1 ± 1	34.2 ± 3.7	527.2 V 102.5 SS	39.4 ± 1	68.0 ± 1.9	527.2 V 102.5 SS	59.0 ± 1	98.5 ± 1.9
Mo	646.6	-4.2 ± 1	-6.5 ± 1.5	1279.8	51.1 ± 1	39.9 ± 0.8	1279.8	81.4 ± 1	62.8 ± 0.8
S[1]	99.8 S 51.0 SS	-8.6 ± 1	-86.2 ± 10	199.8 S 102.2 SS	17.2 ± 1	68.5 ± 5.0	199.8 S 102.2 SS	28.1 ± 1	105.3 ± 5.0
S[2]	63.1 S 56.2 SS	-4.25 ± 1	-66.7 ± 16	63.1 S 56.2 SS	5.6 ± 1	57.9 ± 16	-	-	-
Ta	497.4 Ta 51.4 SS	-27.8 ± 1	-55.7 ± 2.0	1004.4 Ta 102.4 SS	-6.7 ± 1	-10.2 ± 1	1004.4 Ta 102.4 SS	23.0 ± 1	15.9 ± 1.0
C (Graphite)	104.2	19.75 ± 1	189.7 ± 9.6	104.2	27.2 ± 1	260 ± 9.6	196.4	75.2 ± 1	383 ± 5.0
Th	768.2	-12.3 ± 1	-16.0 ± 1.3	1511.7	20.6 ± 1	13.6 ± 0.7	1511.7	40.7 ± 1	26.9 ± 0.7
$B_4^{10}C$	16.1	-64.6 ± 1	-4000 ± 62	16.1	-20.9 ± 1	-1298 ± 62	32.2	-42.0 ± 1	-1305 ± 31
CH_2	14.6	86.7 ± 1	5940 ± 69	14.6	18.9 ± 1	1295 ± 69	29.2	52.6 ± 1	1800 ± 34
Be	120.0	77.7 ± 1	647 ± 8.3	120.0	43.8 ± 1	365 ± 8.3	240.0	126.3 ± 1	526 ± 4.2

(1) Original sulphur sample in ZPR-III inventory.

(2) Sample supplied by W. Y. Kato from ZPR-VI inventory. Suspected impurities in one or the other of these S samples have not been resolved.

(3) Corrected for substances other than materials listed in Column 1.

(4) Worth of sample with all plutonium isotopes present.

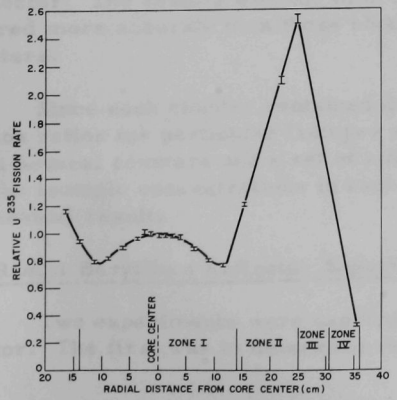

Fig. 18

U^{235} Radial Fission Traverse

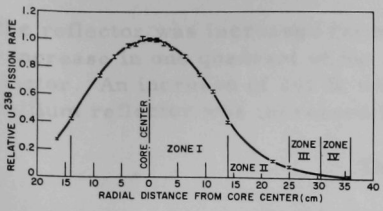

Fig. 19

U^{238} Radial Fission Traverse

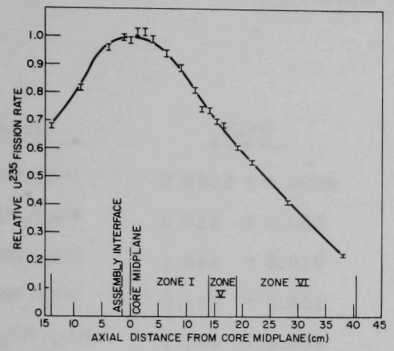

Fig. 20. U^{235} Axial Fission Traverse

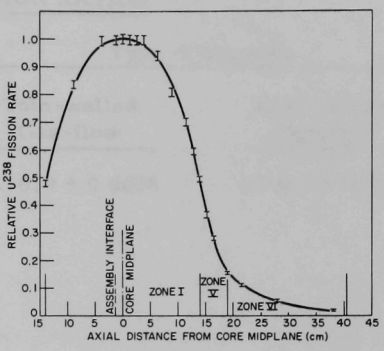

Fig. 21. U^{238} Axial Fission Traverse

There is reason to believe that the wall thickness of the stainless steel-bodied Kirn counters and the proximity of the polyethylene-insulated voltage cable introduces some spectral degradation which affects the measured threshold detector ratios. Consequently, additional measurements were made with the aid of gas-flow counters.(4) Two gas-flow counters have been constructed that allow interchange of fissionable platings on thin steel foils: one with thick-wall construction similar to the Kirn counters, and one with thin walls that uses an extended voltage connector. The results with the thin-walled gas-flow counter are considered more accurate than those obtained with the heavier-walled counters.

Since each counter contained differing amounts of several isotopes, fission ratios for particular isotopes were calculated from data obtained from several counters and a set of simultaneous linear equations involving the isotopic concentrations in each counter. Table VI lists the experimental results.

E. Radial Beryllium Reflector Experiments

Two experiments were carried out with the radial beryllium reflector. The first was to determine the increase in reactivity if the length

of the reflector was increased from 11 to 13 in. This was done by making the increase in one quadrant of the reflector and extrapolating to the entire reflector. An increase of 245 Ih would be obtained if the entire radial beryllium reflector was increased in length from 11 to 13 in.

Table VI

CENTRAL FISSION RATIOS

Ratio	Kirn	Type of Counter: Thin-walled Gas-flow	Type of Counter: Thick-walled Gas-flow
U^{238}/U^{235}	0.0922 ± 0.0006	0.1019 ± 0.0006	0.0963 ± 0.0006
U^{234}/U^{235}	0.522 ± 0.003		
U^{233}/U^{235}	1.544 ± 0.010		
U^{236}/U^{235}	0.195 ± 0.001		
Pu^{239}/U^{235}	1.244 ± 0.008		
Pu^{240}/U^{235}	0.569 ± 0.004		

It was also desired to know the effectiveness of the radial beryllium reflector as a mechanism for reactor control. This control would be obtained by movement of the entire reflector in the axial direction. Therefore, one quadrant of the reflector was moved in 1-in. increments and the results extrapolated to include the entire reflector. These results are shown in Fig. 22.

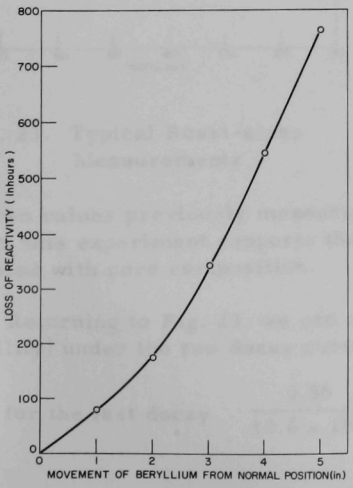

Fig. 22

Worth of Radial Beryllium Reflector Movement

F. Rossi-alpha Measurements

Based on experience with Assembly 19 (a coupled fast-thermal system), it was anticipated that two different values would be observed for the Rossi-alpha in Assembly 40. Consequently, a 9-channel time analyzer with a 2-μsec channel width was used to investigate the expected larger alpha and a 20-channel, 10-μsec width analyzer was used to measure the smaller alpha. Counts from two BF_3 proportional counters (loaded in the P-15 and N-17 matrix positions, see Fig. 2) were alternately used as inputs for the two analyzers. The same counter was used for the initiating or terminating signal on both analyzers.

Typical results of data combined from both analyzers are shown in Fig. 23. The measured values of Rossi-alpha, averaged from several runs similar to those shown in Fig. 23, are $(-10.9 \pm .7) \times 10^4$ and $(-8.8 \pm .2) \times 10^3$ sec^{-1}. The larger alpha (faster decay) is interpreted as representing the time behavior of chain-related coincident neutron pairs having no intervening links in the beryllium reflector (i.e., it is the alpha representative of the core composition). The smaller alpha (longer decay) represents the time behavior of chain-related coincident neutron pairs when at least one intervening event has occurred in the beryllium.

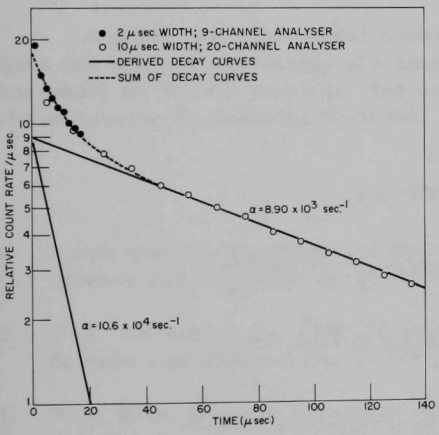

Fig. 23. Typical Rossi-alpha Measurements

A supplementary measurement was made with the terminating counter in the L-20 location in the beryllium reflector. In this configuration, the terminating neutron must almost certainly be related to the initiating neutron of the coincident pair through events occurring in the beryllium. This time, a single value for alpha was obtained, agreeing with the smaller of the two values previously measured. The disappearance of the fast decay in this experiment supports the hypothesis that the large alpha is associated with core composition.

Returning to Fig. 23, we can see that the total areas (integrated probability) under the two decay curves are:

$$\text{for the fast decay} \quad \frac{0.86}{10.6 \times 10^4} = 0.081 \times 10^{-4}$$

and,

$$\text{for the slow decay} \quad \frac{0.89}{8.9 \times 10^3} = 0.10 \times 10^{-3}$$

This indicates that, if the analyzer sees two chain-related neutrons in the center of the core, the chances are greater than 10 to 1 that there will have been intervening events in the beryllium. This preponderance of the slower decay scheme makes it reasonable to assign it as an approximate weighted average behavior to the reactor as a whole. This then gives an estimated lifetime of

$$\ell = \frac{\beta}{\alpha} = \frac{0.0068}{8.8 \times 10^3} = 7.7 \times 10^{-7} \text{ sec} \quad .$$

ACKNOWLEDGMENTS

A great deal of time and effort were spent in the theoretical calculations and preliminary design of a small, lightweight fast reactor of which Assembly 40 was the mockup. The credit for this work goes to K. K. Almenas of the Reactor Engineering Division.

REFERENCES

1. Ralph Cooper, Fast Reactor Rocket Engines - Criticality, Nuclear Science and Engineering, 13, 355-365 (1962).

2. B. C. Cerutti et al., ZPR-III, Argonne's Fast Critical Facility, Nuclear Science and Engineering, 1, 126 (1956).

3. F. S. Kirn, Neutron Detection with an Absolute Fission Counter, Paper SM-36/74 presented at Symposium on Neutron Detection, Dosimetry and Standardization, IAEA, Harwell, England (Dec 1962).

4. W. G. Davey, A Critical Comparison of Measured and Calculated Fission Ratios for ZPR-III Assemblies, ANL-6617 (Sep 1962).